Available online at www.sciencedirect.com
ScienceDirect
Sedimentary Geology 195 (2007) 239–256
Sedimentary Geology
www.elsevier.com/locate/sedgeo

Giant earthquakes in South-Central Chile revealed by Holocene mass-wasting events in Lake Puyehue

Jasper Moernaut [a,*], Marc De Batist [a], Francois Charlet [a], Katrien Heirman [a], Emmanuel Chapron [b], Mario Pino [c], Robert Brümmer [c], Roberto Urrutia [d]

[a] *Renard Centre of Marine Geology (RCMG), Ghent University, Krijgslaan 281, 9000 Ghent, Belgium*
[b] *Geological Institute, ETH Zurich, Sonneggstr. 5 CH-8092 Zurich, Switzerland*
[c] *Instituto de Geociencias, Universidad Austral de Chile, Casilla 567, Valdivia, Chile*
[d] *Centro EULA, Universidad de Concepción, Casilla 160-C, Concepción, Chile*

Received 19 April 2006; received in revised form 24 August 2006; accepted 25 August 2006

Abstract

Very high resolution reflection seismic profiling (3.5 kHz) revealed nine Holocene mass-wasting events in Lake Puyehue (South-Central Chile). These events are made up of numerous coeval mass-wasting deposits and some homogenites, which are radiocarbon-dated. The two youngest mass-wasting events could be attributed to the giant AD 1960 and AD 1575 Valdivia earthquakes. The most extensive event took place around 1660 cal yr BP. Evaluation of all possible slope failure processes led us to infer that giant earthquakes, roughly comparable to the AD 1960 Valdivia earthquake (M_w=9.5), are the most likely trigger mechanisms of all mass-wasting events in Lake Puyehue. These occurred with a mean recurrence rate of 1000 yr although relatively aperiodically (ranging between 500 and 2000 yr). Quantitative comparison of mass-wasting events related to historically reported earthquakes (AD 1960 and AD 1575) showed significant differences although these earthquakes are assumed to have had a comparable strength. A lowered background sedimentation rate could be responsible for this variable earthquake recording, which highlights the importance of a thorough assessment of the depositional history before using lacustrine records for quantitative paleoseismic analysis.

Keywords: Lake sediments; Mass-wasting; South-Central Chile; Holocene; Giant earthquakes

1. Introduction

Strong seismic ground shaking is well known to be capable of triggering liquefaction structures, soft-sediment deformation and simultaneous slope failures, in sub-aerial and sub-aqueous environments. Onshore *in situ* liquefaction structures and soft-sediment deformation are widely acknowledged as indicators of past seismic events and can even provide estimations of paleo-earthquake epicenters and magnitudes (Ishihara, 1985; Obermeier, 1996; Green et al., 2005). Earthquakes as small as M_l=4 can produce landslides, but stronger earthquakes can initiate widespread and abundant landslides over large areas and of various type, strongly affecting drainage basins and sediment generation (Keefer, 1984; Keefer, 1999). Unfortunately, the paleoseismological use of subaerial slope failures (Jibson, 1996; Becker and Davenport, 2003) is restricted due to difficulties in determining age, erosion and

* Corresponding author. Tel.: +32 9 2644637; fax: +32 9 2644967.
E-mail address: Jasper.Moernaut@UGent.be (J. Moernaut).

0037-0738/$ - see front matter © 2006 Elsevier B.V. All rights reserved.
doi:10.1016/j.sedgeo.2006.08.005

speculative estimations of the causal slope-failure mechanism (e.g. earthquakes, rainfall).

In subaqueous environments, triggering of slope failures is more difficult because driving forces must be large enough to overcome the effect of hydrostatic loading, a stabilizing factor against slope instability. Thus, higher seismic intensities are needed to effectively trigger mass-movements. However, pore-water overpressure (undercompaction) due to rapid sedimentation or the presence of permeability barriers can significantly decrease the stability of submerged slopes. The high resolution and often easily datable sedimentary archives in lake basins can provide a good record of paleoseismic activity if clear coseismic features are induced, preserved and characterized. Synchroneity of such features at different locations is the major criterion to postulate seismic triggering (Jibson, 1996; Ettensohn et al., 2002). Lacustrine sedimentary archives have been utilized in paleoseismological research for several decades (e.g. Sims, 1975; Doig, 1986; Inouchi et al., 1996). Historical earthquakes (M_w=5 to 7) are known to have triggered coseismic sediment disturbances in several Alpine lakes (Nomade et al., 2005). These studies suggest that *in situ* soft-sediment deformation starts at intensities VI–VII and multiple slope failures become more frequent at higher intensities (Monecke et al., 2004). In Lake Lucerne (Switzerland), sub-bottom acoustic profiles were used to identify earthquake-induced slumps, revealing prehistorical earthquake activity (Schnellmann et al., 2002). Some of these paleo-earthquakes (and/or sub-aquatic mass-movements) can also induce lake-water oscillations (seiches), such as the one that damaged the city of Lucerne and caused the accumulation of up to 3 m of homogeneous mud on the basin plain (Siegenthaler et al., 1987). Lacustrine paleoseismic investigation combines high-resolution seismic reflection profiles and sediment coring. Seismic profiles are essential for identifying and locating multiple mass-wasting deposits and for evaluating their synchroneity. Sediment cores are used for ground-truthing seismic profiles and to provide an age model (based on ^{14}C dating, varve-counting, etc.) necessary to date paleoseismic events. Coring further allows evaluation of the hypothesized earthquake triggering through correlation of historically well-reported seismic events with visible sedimentary features.

Paleoseismological research in Chile is relatively new, despite the fact that the region's high historical seismicity and locally dense population demand a precise seismic hazard assessment. In South-Central Chile, uplifted beach berms and coastal deformation have been investigated on Santa María Island (Bookhagen et al., 2006; Melnick et al., in press), buried soils and tsunami deposits at Río Maullín estuary (Cisternas et al., 2005), marine turbidites offshore Valdivia (Blumberg et al., personal communication), and mass-wasting processes in Lake Icalma (Bertrand et al., in press).

In the present paper, we make a first attempt to reconstruct the earthquake history for the area around Lake Puyehue (40°S) in South-Central Chile, principally based on a study of high-resolution seismic reflection profiles and their correlation with an existing age model for Lake Puyehue's sediments. We will show that Lake Puyehue bears a valuable paleoseismic record, evidenced by multiple seismically triggered mass-wasting events during the Holocene.

2. Study area

2.1. General setting of South-Central Chile

The regional tectonic setting (Fig. 1A) of our study area in South-Central Chile is dominated by the slightly oblique subduction of the Nazca Plate under the South American Plate, with a convergence rate of about 8 cm/yr towards N78°E (De Mets et al., 1994). The subducting oceanic slab is characterized by prominent along-strike variations in dip angle and defines, in our study area, a 30°E-dipping plane (Bohm et al., 2002). The Mocha Fracture Zone and the Valdivia Fracture Zone delineate oceanic lithospheres of different age at the subduction trench: at least 35 Ma north of 38°S and less than 20 Ma south of 40°S (Müller et al., 1997). The Liquiñe–Ofqui Fault Zone (LOFZ), a long-lived (since the Eocene) dextral strike–slip lineament, mostly accommodates the stress generated by the oblique subduction (Cembrano et al., 2000). Several NW–SE trending fault zones constitute first-order discontinuities in the overriding plate which separate different metamorphic and magmatic segments (Rapela and Pankhurst, 1992; Lavenu and Cembrano, 1999).

The Andean margin between 36°S and 42°S consists of three main geomorphological units: (from W to E) the Coastal Range, the longitudinal Central Valley and the main Andean Cordillera (Fig. 1A). The Coastal Range is composed of a Late Paleozoic accretionary prism and magmatic arc (Willner et al., 2004). The Central Valley consists of Eocene–Miocene volcano-sedimentary deposits (Jordan et al., 2001), which are overlain by Pliocene–Quaternary volcanics and volcaniclastics, and fluvial and fluvioglacial deposits. The main Andean Cordillera gives rise to the present-day volcanic arc, mainly aligned along the prominent Liquiñe–Ofqui Fault Zone (Cembrano et al., 2000). This volcanic arc is

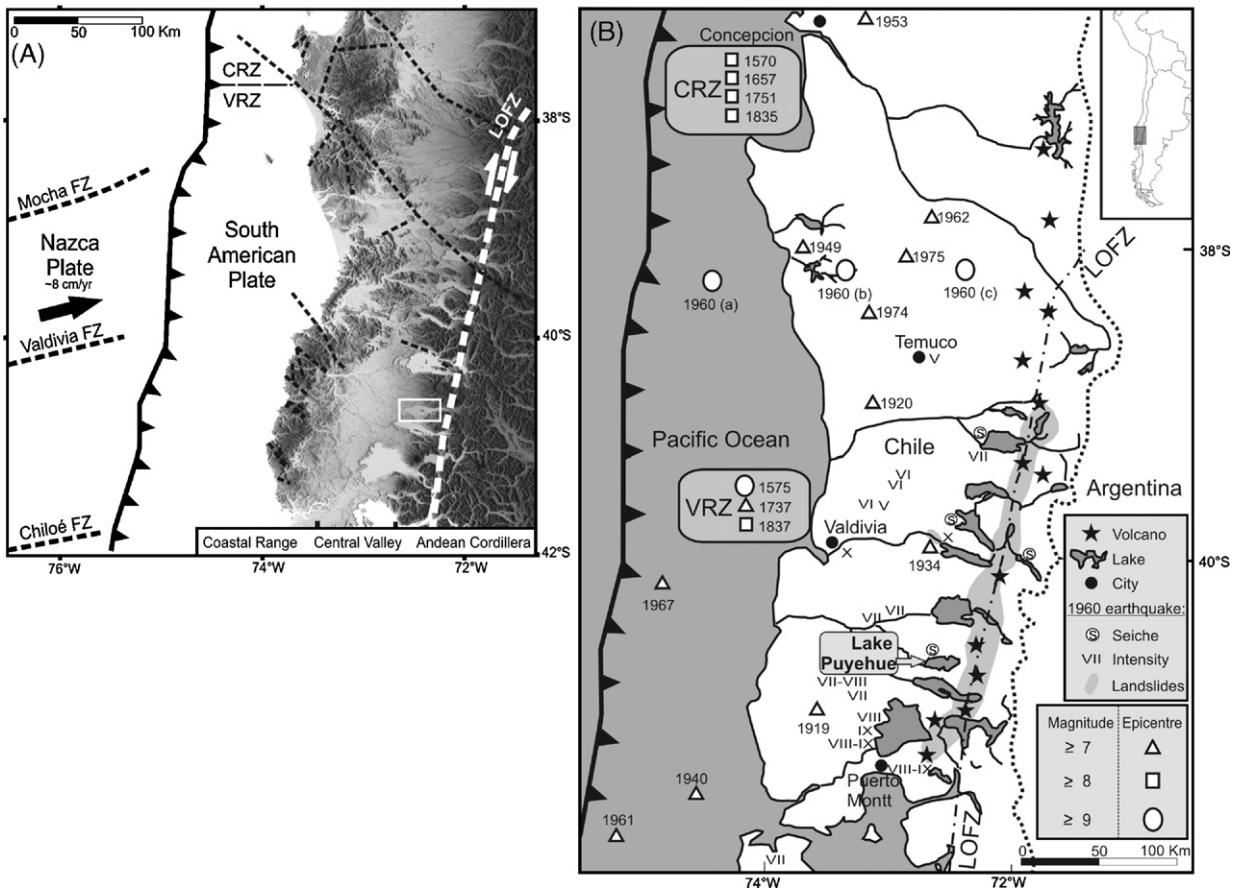

Fig. 1. (A) DEM of South-Central Chile (SRTM data) showing the main geomorphic features: the Coastal Range, the Central Valley and the main Andean Cordillera. Oblique subduction of Nazca Plate under South American Plate: trench location modified from Melnick et al. (in press). FZ=fracture zone. CRZ: Concepcion rupture zone; VRZ: Valdivia rupture zone. Onshore faults are derived from Lavenu and Cembrano (1999), Bohm et al. (2002) and the geological map produced by SERNAGEOMIN (2003). LOFZ=Liquiñe–Ofqui Fault Zone. Location of Lake Puyehue is indicated by a white rectangle. (B) Earthquake occurrence in South-Central Chile and selection of reported impacts of the giant AD 1960 earthquake. AD 1960 earthquake impact: Grey shaded area represents the landsliding-affected zone (modified from Chapron et al., in press). Lake seiche reports from Sievers (2000). Modified Mercalli Intensity from Duke and Leeds (1963). Historical earthquake data compiled from Kelleher (1972), Lomnitz (1970, 2004), websites: USGS (http://neic.usgs.gov/neis/epic) and Servicio Sismologico Universidad de Chile (http://ssn.dgf.uchile.cl/home/terrem.html). Three different epicenter locations of the AD 1960 earthquake are mentioned in recent literature (Lorenzo-Martin et al., 2006, and references therein).

part of the Southern Volcanic Zone (SVZ) of the Andes, where volcanic activity has been intensively studied (summarized in Stern, 2004).

Strong to very strong (M_w>8) historical subduction earthquakes have affected the region (Fig. 1B). Most were accompanied by noticeable coastal elevation changes and, depending on the amount of vertical sea-floor displacement, catastrophic tsunamis. Their rupture zones are limited to the coupled region between the Nazca and South American plates, which extends to about 60 km depth (Pardo et al., 2002). The most impressive event is definitely the 1960 Valdivia earthquake (M_w=9.5), the largest instrumentally recorded earthquake ever, with a rupture length of about 1000 km (Cifuentes, 1989). It induced coseismic vertical land movements of up to 6 m (Veyl, 1961) and a giant tsunami that even damaged the coast of Japan (Lomnitz, 2004). Within our study area, it triggered numerous landslides in the Golgol Valley (Chapron et al., in press) and a fissure eruption of the Cordon Caulle volcanic complex, clearly illustrating the relationship between seismo-tectonics and volcanic reactivation (Lara et al., 2004). Chapron et al. (in press) provides a summary of the subaqueous and subaerial sedimentary traces of the impact of the 1960 earthquake in Chile and Argentina (39–43°S). Lake Puyehue is located in the vicinity of

the Valdivia rupture segment, which has experienced four major earthquakes (AD 1575, 1737, 1837, 1960) since the arrival of the Spanish around AD 1535 (Lomnitz, 2004). Note that pre-instrumental earthquake archives are incomplete and may have been constructed from uncertain intensity and epicentre estimations. It is also important to note that the recurrence intervals of giant earthquakes with rupture lengths of about 1000 km may be so large that very few have been recorded in historical times (Cifuentes, 1989), which therefore makes the AD 1960 earthquake appear unique. The only comparable historical event is the well-documented AD 2004 Sumatra–Andaman earthquake (M_w=9.3), which had a larger rupture length (~1300 km) but smaller slip area (Ishii et al., 2005).

The high seismicity of the Chilean convergence zone indicates episodic and discrete absorption of the oceanic plate (Stauder, 1973). All of the plate convergence along this part of the Chilean trench is currently accommodated by the build-up of elastic strain, which leads to a high probability of future giant earthquakes (Klotz et al., 2001). A statistical evaluation of the seismic potential for large interplate earthquakes in Chile has been established from historical datasets (Nishenko, 1985), but a larger paleo-earthquake dataset is indispensable for accurately determining giant earthquake recurrence rates.

2.2. Lake Puyehue: location and setting

Lake Puyehue (40°40′S; 72°28′W) is situated in the Lake District (37°S–42°S) of South-Central Chile, at the western foot of the Andes (Fig. 1A). This region has been strongly influenced by the interaction between volcanism, tectonics, seismic activity and Pleistocene glaciations, all leaving a distinct imprint on a continually evolving landscape.

Lake Puyehue (Fig. 2) is an oligotrophic and temperate monomictic lake situated at 185 m asl with a surface area of 165.4 km^2 and a water volume of 12.6 km^3 (Campos et al., 1989). It was formed by glacial-valley overdeepening during the Late Quaternary glaciations and subsequent moraine-damming of its borders (Laugenie, 1982). Its outlet cross-cuts several of these moraine ridges (Bentley, 1997), and ultimately flows westward into the Pacific Ocean. Lake Puyehue's catchment mainly consists of Quaternary volcanic rocks covered by post-glacial andosols and has a surface of 1431 km^2 (Bertrand, 2002). The Golgol River is the main affluent (Campos et al., 1989), forming an alluvial plain probably filling up the eastern part of a former Puyehue lake extension. The Lican River forms a small but distinct delta plain in the northern part of Lake Puyehue. Several Quaternary volcanoes surround its watershed, such as the Puyehue–Cordon Caulle (2240 m) and Casablanca (1990 m) volcanic complexes (Gerlach et al., 1988).

The bathymetric map (Fig. 2C) clearly shows three sub-basins in Lake Puyehue, shallowing to the west. The Western and Northern Basins are separated by a lake-crossing ridge, which is interpreted as the continuation of an onshore moraine (Bentley, 1997; Heirman, 2005). The Eastern Basin constitutes the deepest part of the lake (max. 123 m). A steep-sloped (25°–30°) ridge-and-platform morphology limits the eastern part of the Eastern Basin. A gully depression is located between Fresia Island and an elevated platform in the south (coring site PU-II).

3. Methodology

3.1. Reflection seismic data

After an initial high-resolution sparker seismic reconnaissance survey (austral summer 2001–2002), Lake Puyehue was studied in more detail with a very high resolution GEOPULSE pinger system (austral summers of 2001–2002 and 2004–2005). The seismic source/receiver was mounted on a Cataraft system that was towed by the Huala II, the small scientific vessel from the Universidad Austral de Chile. The acoustic signal, with a central frequency of 3.5 kHz, penetrated the upper 20–25 ms TWT (15–20 m) of the sedimentary fill with a resolution of about 25 cm. Navigation and positioning was achieved by GPS. All data were recorded digitally on a TRITON–ELICS Delph-2 acquisition system. The study area, focusing on the Eastern Basin and the southern elevated platform, was covered with a grid of more than 150 km of seismic lines (Fig. 2B).

Data processing, including band-pass filtering, scaling and spiking deconvolution, was carried out on a LANDMARK ProMax system and seismic stratigraphic interpretation was done using SMT's Kingdom Suite package. Water depths were calculated using a mean velocity of 1470 m/s, derived from correlation between core depths and adjacent seismic profiles.

3.2. Sediment cores

In the austral summer of 2001–2002, two long piston cores (PU-I and PU-II; Bertrand, 2005) were retrieved using the UWITEC coring platform from the University of Savoie. The coring sites (location: Fig. 2C) were selected in the framework of a paleoclimatological investigation and based on the results of the seismic reconnaissance. Magnetic susceptibility and gamma density were measured on whole-round cores with a

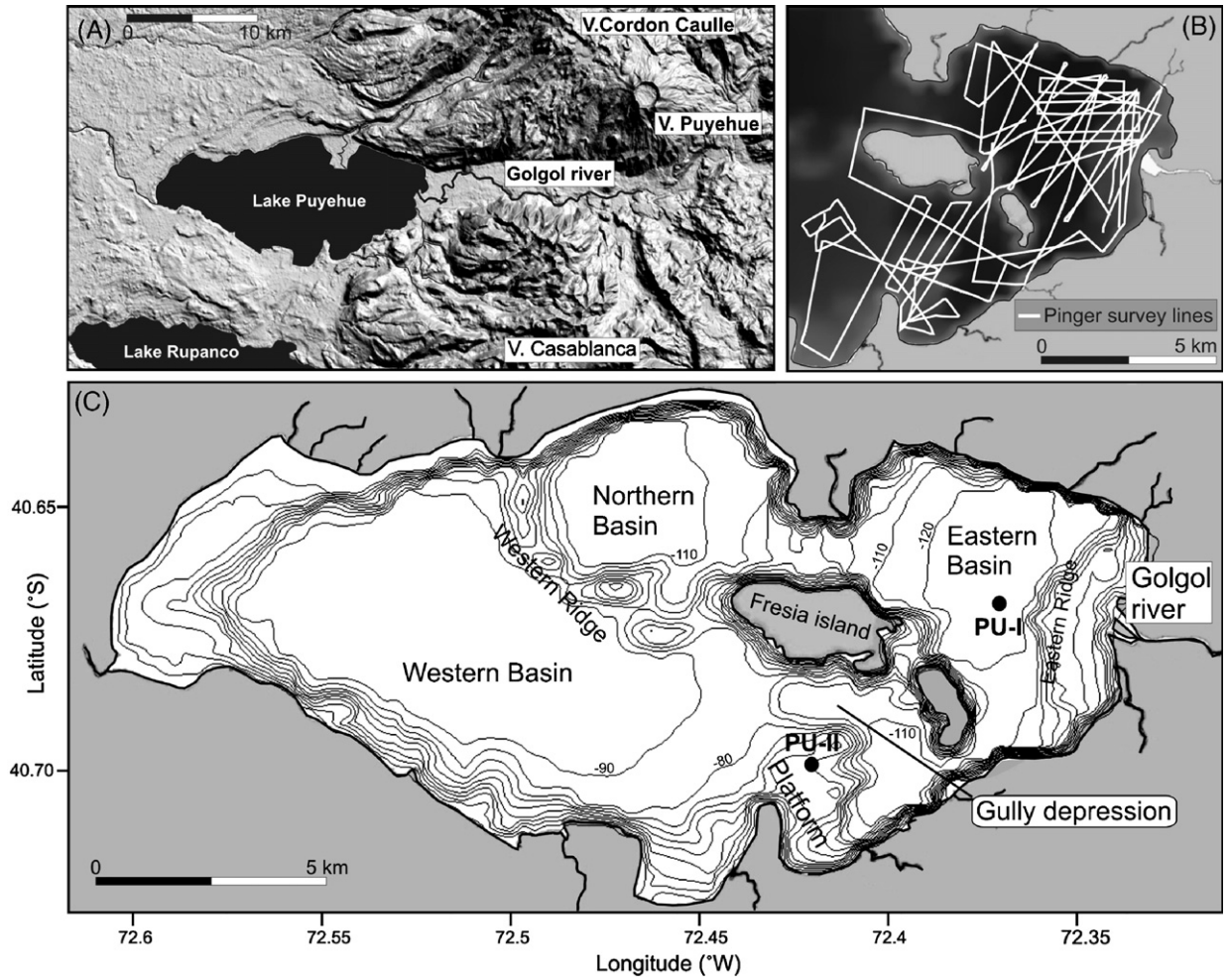

Fig. 2. (A) DEM of the area around Lake Puyehue (SRTM-data). Note two important volcanic complexes in its drainage basin (Puyehue–Cordon Caulle, Casablanca). The Golgol River is the main affluent in Lake Puyehue's drainage basin. (B) Location of pinger survey lines. (C) Geomorphological units in Lake Puyehue. Bathymetry obtained by interpolation between seismic profiles (Moernaut, 2005). Isobaths every 10 m. Coring sites PU-I and PU-II are indicated.

GEOTEK multi-sensor core logger. P-wave velocity could not be measured due to the presence of vacuums in the cores. Subsequently, the cores were split, photographed and described macroscopically. Core-to-core correlation was achieved by comparing both visual characteristics and petrophysical signatures (Bertrand, 2005).

4. Mass-wasting deposits in the seismic stratigraphy of Lake Puyehue

The 2001 seismic sparker profiles (Charlet et al., submitted for publication) imaged the entire lacustrine infill of the Western Basin of Lake Puyehue, down to the substratum, and permitted establishment of a seismic stratigraphy (Fig. 3). Five major seismic sequences (U1–U5, from bottom to top) make up the sedimentary infill, with an overall maximum thickness of 210 m (Charlet et al., submitted for publication). These seismic units represent the evolution of the sedimentary environment from the onset of the last deglaciation until the present, with U1 representing moraine deposits, U2 and U3 glaciolacustrine deposits, U4 fluvial-dominated lacustrine deposits and U5 open lacustrine deposits (Charlet et al., submitted for publication; Heirman, 2005).

In this study, we only used the pinger profiles, as they provide the detail (about 25 cm resolution) required for the analysis of mass-wasting deposits. The penetration of these 3.5 kHz seismic profiles is usually limited to about 15–20 m sub-bottom depth, i.e. seismic sequence U5 and the uppermost part of U4 on the southern

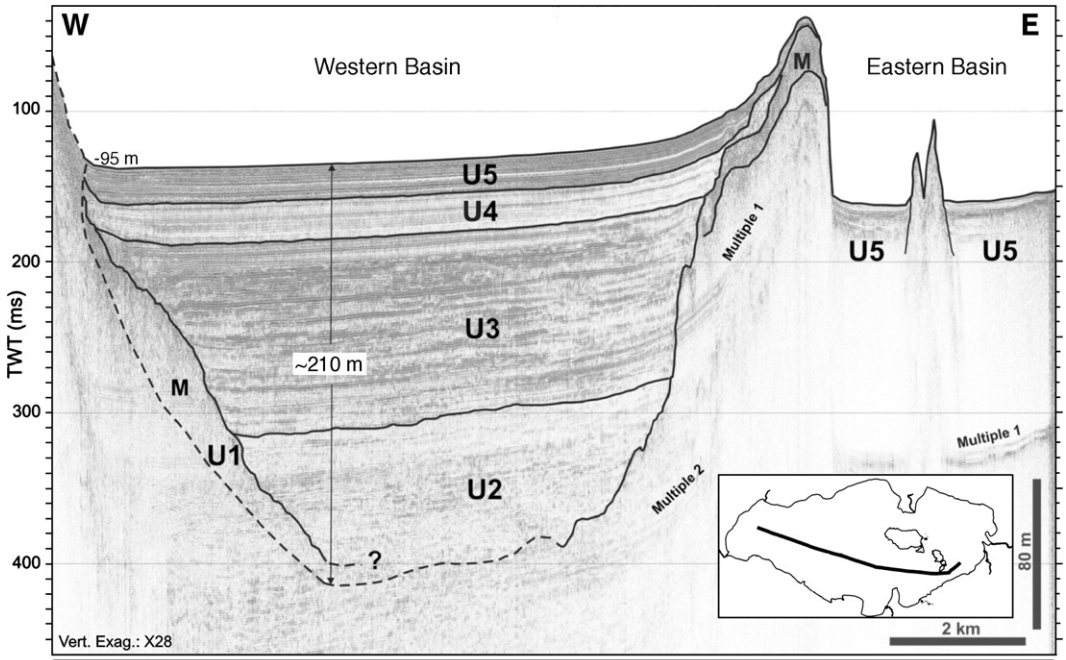

	Seismic facies	Interpretation
Unit 5	Drape of parallel continuous high-amplitude reflectors	Open lacustrine hemipelagic deposits
Unit 4	Low to medium-amplitude reflectors	Glaciolacustrine deposits
Unit 3	Infill of parallel, medium to high-amplitude reflectors interrupted by chaotic lenses	Fluvio-glacial deposits with outwash channels
Unit 2	Infill of chaotic, reflection-free to irregularly stratified facies with low-amplitude reflectors	Glaciolacustrine deposits during initial glacier retreat (ice-contact)
Unit 1	- Transparent to chaotic high-amplitude reflectors overlain by irregularly stratified reflectors - 2 isolated bodies: on deep slope of rocky substratum and on Western Ridge	Moraine deposits

Fig. 3. General seismic stratigraphy of Lake Puyehue (Charlet et al., submitted for publication) based on sparker seismic profiles. Five seismic units (U1–U5) can be discerned in the Western Basin, while the acoustic penetration in the Eastern Basin is limited to the upper part of U5. M=morainic deposit. Inset figure: localization of the sparker profile.

platform. Sequence U4 is acoustically stratified and its seismic facies comprise low-amplitude reflections with an onlapping, infilling geometry. Sequence U5 is highly stratified and mostly consists of continuous, high-amplitude reflections in a draping configuration (Charlet et al., submitted for publication).

Locally, however, the well-stratified facies of U5 is disrupted by lenses with a chaotic to transparent facies. These lenses are of variable geometry and are concentrated along the slope margins. Representative examples are shown on Fig. 4. Lenses c and d are elongate in comparison to lenses a and b (lengths vary between about 80 and 300 m). Thickness of all these lenses is about 1.5 ms (~1.20 m). The acoustic facies of lenses a and d is more or less transparent, whereas lenses b and c are characterized by a more chaotic seismic facies.

These lenses are interpreted as mass-wasting deposits (MWD), resulting from underwater slope failures and subsequent mass-movement processes (e.g. Schnellmann et al., 2002). Slope instabilities have been initiated on slope angles ranging from 4° to 25°. After emplacement, these MWD have been buried by the draped units of sequence U5, which represent the open lacustrine background sedimentation. The uppermost mass-wasting deposit has to be of quite recent origin as it occurs virtually at the surface. Variations in geometry of the MWD possibly reflect differences in dynamic characteristics of the original mass-movement process (e.g. flowing versus sliding). Mass-wasting deposits must have a thickness of at least 40–50 cm to be illustrated on pinger seismic profiles because of the ±25 cm pinger seismic resolution. As a consequence, many mass-wasting deposits are too small to be resolved on seismic images (bed thickness <40 cm). Accurate 3D-mapping and volume calculation of the mass-wasting deposits was not possible, as the seismic grid is still too wide compared to their lateral extent.

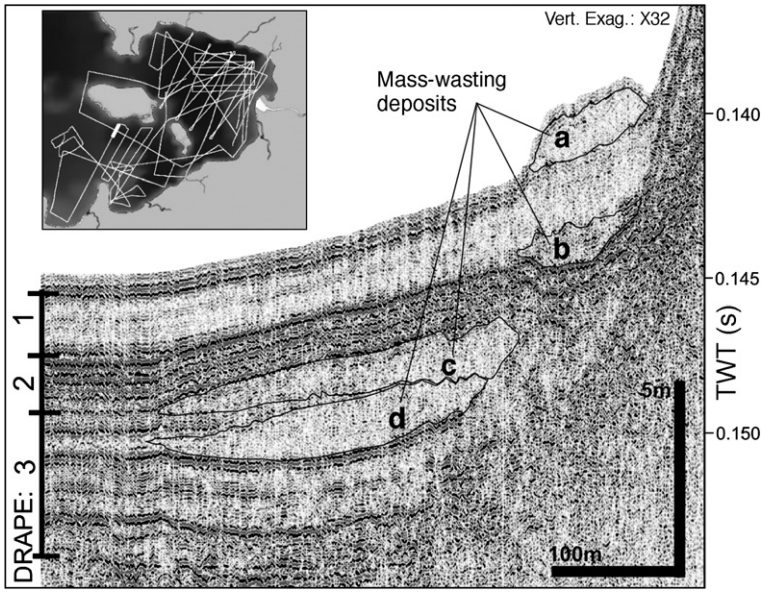

Fig. 4. Reflection seismic evidence for lacustrine mass-movements: well-stratified background sedimentation drape (1–2–3) and 4 intercalated lenses (mass-wasting deposits: a–b–c–d) at the N-slope margin of the gully depression.

As a generally accepted classification for lacustrine mass-wasting deposits based on their appearance on seismic profiles is still lacking, this has resulted in the past years in arbitrary nomenclature and consequent confusion in the international literature. In this article, we will use the general term "mass-wasting deposit" for deposits resulting from all kinds of sub-aqueous slides, slumps, debris flows and debris avalanches.

5. Core PU-II and the core–seismic correlation

Core PU-II (11.22 m long, water depth of 48.4 m) was taken on the southern elevated platform (Figs. 2C and 5). Sparker seismic data show that the coring site is characterized by a moraine substratum (U1) overlain by undisturbed sediments of sequence U4 and U5 (Charlet et al., submitted for publication). The lithology of PU-II is dominated by finely laminated to homogenous silt, mainly composed of diatoms, organic matter, amorphous clays, mineral grains and volcanic glass (Bertrand, 2005). Intercalated in this open lacustrine background sedimentation are 79 coarse-grained tephra layers and 3 thin turbidites, representing a relatively limited clastic influence (4.66%) on the sedimentation at this location.

An age–depth model (Fig. 5) has been established (Bertrand, 2005), based on 9 AMS radiocarbon dates, varve-counting techniques (Boës and Fagel, in press) and correlation of historical volcanic eruptions with tephra layers. Vertical segments represent event deposits such as tephra layers and turbidites (Bertrand, 2005). The age–depth curve yields an extrapolated age for the base of the core of 17,915 cal yr BP. The presence of varve-laminations and an undisturbed seismic–stratigraphic sequence makes the occurrence of significant changes in average sedimentation rate highly unlikely.

Using the pinger seismic data from the southern platform, sequence U5 can be further sub-divided into twelve seismic sub-units (5a to 5l), essentially based on seismic facies characteristics (e.g. continuous high-amplitude reflections, distinct facies transitions). At coring site PU-II, this seismic stratigraphy can be tied to the core lithology (Fig. 5), using an estimated, average acoustic velocity of 1600 m/s, similar to the velocity obtained by seismic refraction measurements on the uppermost seismic unit in the glacigenic Alpine lakes Le Bourget and Annecy (Finckh et al., 1984). Several of the high-amplitude reflections in U5 correlate with coarse-grained event deposits in the core (tephra layers, turbidites). This core-to-seismic correlation allows dating of the key seismic horizons using the above age model. The boundary between U5 and U4 is dated at 23,600 cal yr BP by linear extrapolation. The dated horizons are then extrapolated across the entire pinger grid, leading to a detailed seismic chronostratigraphy for U5 that can be used for dating intercalated mass-wasting deposits. MWD are then dated at their distal parts, where they can be accurately situated in the sequence, by linear

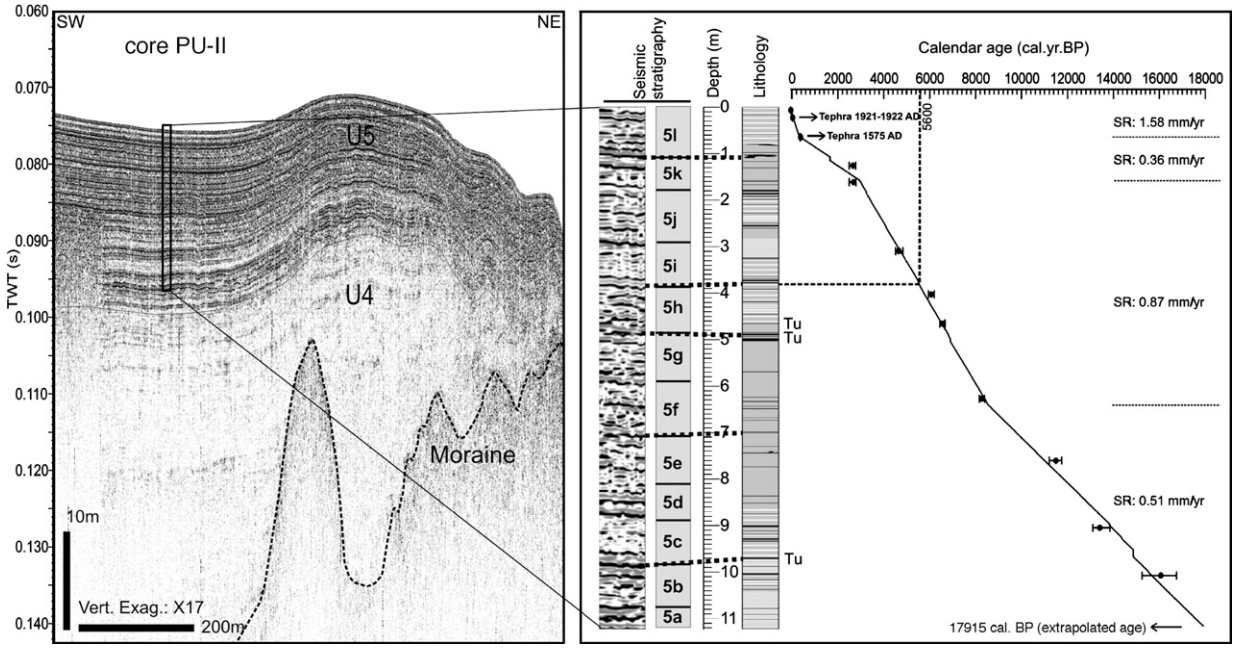

Fig. 5. Coring site PU-II projected on a pinger seismic profile. Correlation between the sedimentary record in core PU-II and the 12 seismic sub-units of seismic unit 5. High-amplitude reflections sometimes correlate with coarse-grained tephra deposits (black lines) or turbidites ("Tu"). Seismic–stratigraphic horizons are dated using the age–depth model of Bertrand (2005). E.g.: 5h–5i boundary is dated at 5600 cal yr. BP.

interpolation between the nearest chronostratigraphic horizons, after removal of obvious event deposits.

6. Mass-wasting events (MWE)

Our study highlights that in Lake Puyehue multiple mass-wasting deposits (MWD) often occur at the same seismic–stratigraphic horizon in different parts of the lake basin. This indicates that they were coeval and that they represent a single mass-wasting event (MWE) of basin-wide importance (e.g. MWD3 on Fig. 6A represents a MWD deposited during MWE3).

Below, we will describe a number of characteristic mass-wasting deposits and date their corresponding mass-wasting event. This description will be made from young to old because of the decreasing age control and acoustic penetration with depth. Analyzing several MWD per event offered an average date for each mass-wasting event in cal yr BP, accompanied by an error derived from ^{14}C dating. The real error bar on our dating will be larger – but difficult to quantify – because of possible core-to-seismic correlation errors and vertical resolution limitations.

Our analysis is restricted to mass-wasting deposits younger than about 10,000 cal yr BP. Older MWDs are also observed, but their use for paleoseismological reconstructions is restricted due to a lack of seismic data, acoustic penetration and accurate age control at these depths.

6.1. MWE1

At least 17 mass-wasting deposits are observed at this seismic–stratigraphic horizon. The most significant MWDs occur at the base of the eastern steep-sloped ridge. This is very likely due to the proximity of the Golgol River, the main source of sediment input in Lake Puyehue, and thus to the availability of sediments prone to failure. Fig. 7A shows the most voluminous mass-wasting deposit (MWD1), which reaches a maximum thickness of 8 m and an apparent length of 500 m. It is characterized by a chaotic facies with a hummocky upper limit. The upper limit can locally be observed below a thin drape of background sediment. The lower limit is only visible in the distal part and is evidenced by a downwarped high-amplitude reflection. This downwarping possibly results from compaction of underlying sediment due to the gravitational loading by the MWD. The continuous high-amplitude reflection at the base of the MWD can be correlated to an abrupt change in bulk density associated with a pumice layer in core PU-I (Chapron et al., in press). Two different core descriptions and age–depth models have been proposed for PU-I (Fig. 7C). Model 1 has been established based on

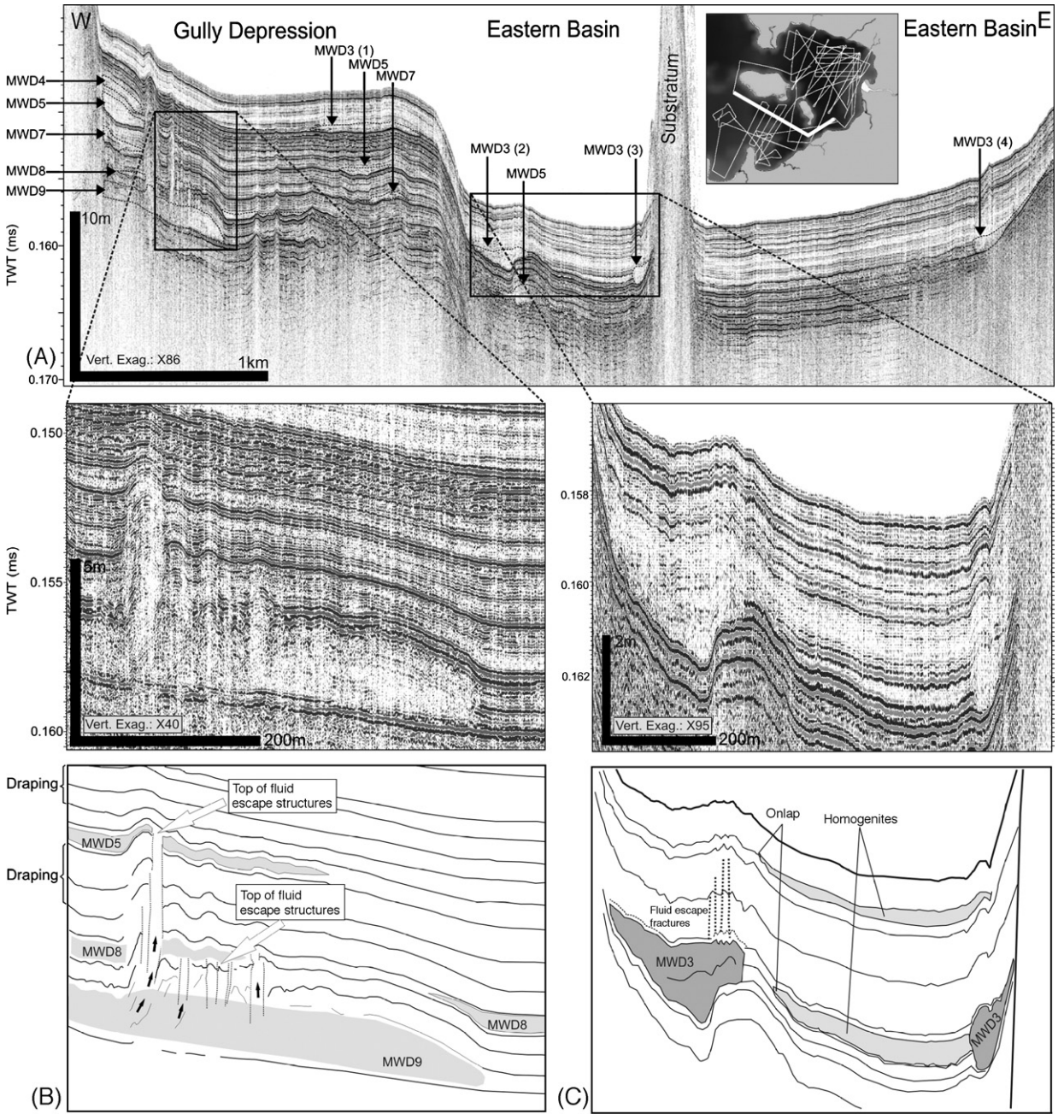

Fig. 6. (A) W–E pinger profile illustrating the seismic stratigraphy of different morphological units in the eastern part of Lake Puyehue. Multiple MWDs are observed at single seismic–stratigraphic horizons (e.g. MWD3 occurs 4 times on this seismic profile). A bold white line on the inset figure illustrates the profile location. (B) Fluid escape structures originating in MWD9: vertical fractures, uplifted stratification and breached stratigraphic horizons. The top of these structures can be linked to mass-wasting deposits. (C) 2 MWDs at the same seismic–stratigraphical level, representing MWE3. Vertical fluid-escape fractures occur in the most western MWD. These MWDs are associated with an onlapping transparent lens, interpreted as a homogenite. The uppermost homogenite is at the MWE1 stratigraphic level.

varve-counting techniques and recognition of sedimentary events (Boës and Fagel, in press). In this model, the pumice layer has an age of AD 1834–37. Model 2 has been established using radionuclide data, recognition of sedimentary events and tephrostratigraphy (Chapron et al., in press). The pumice layer is interpreted to mark the base of a mega-flood deposit dated at AD 1960.

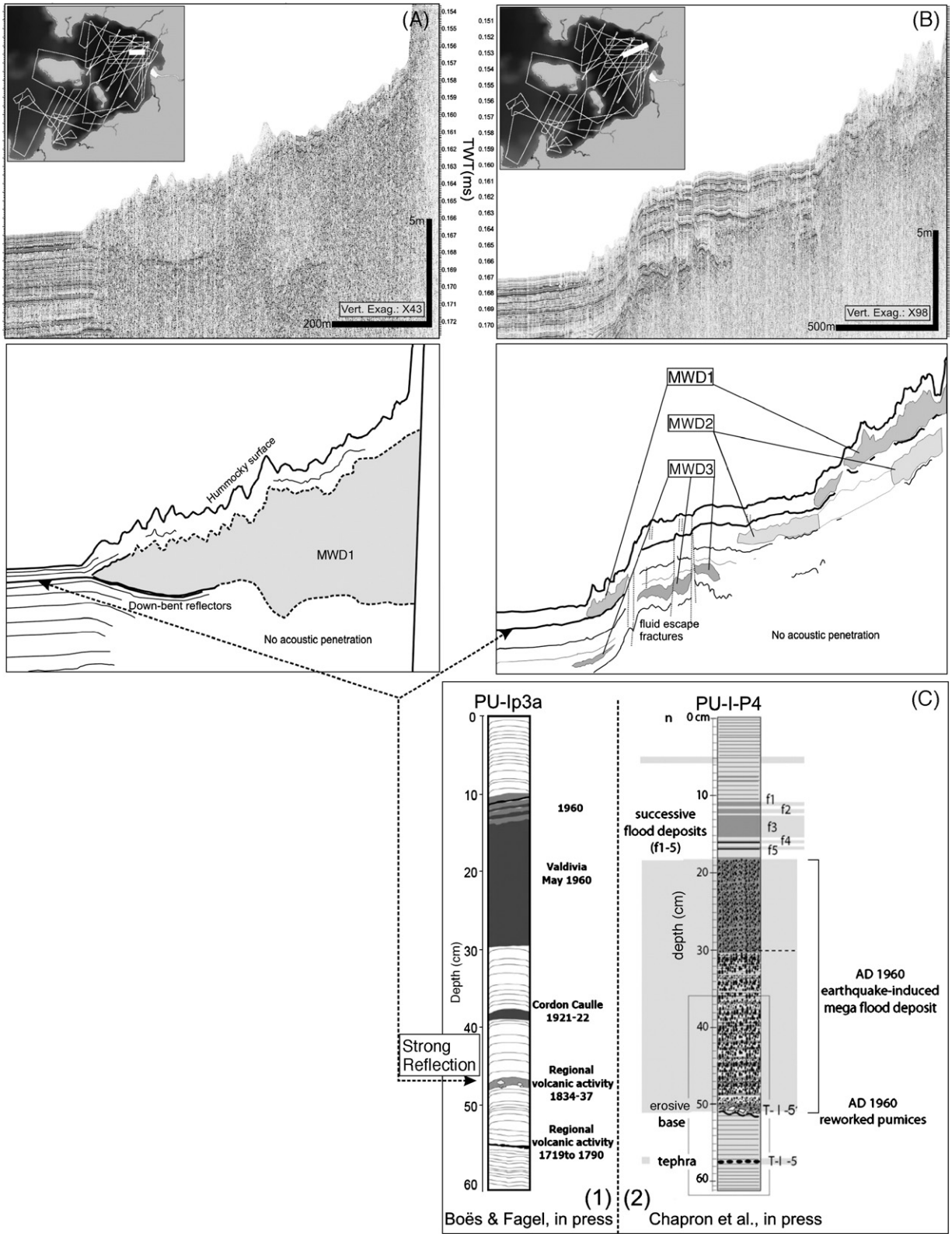
(A)
(B)
TWT (ms)
5m
Vert. Exag.: X43
200m
Vert. Exag.: X98
500m
Hummocky surface
MWD1
Down-bent reflectors
No acoustic penetration
MWD2
MWD3
fluid escape fractures
PU-Ip3a
PU-I-P4
(C)
Depth (cm)
1960
Valdivia May 1960
Cordon Caulle 1921-22
Regional volcanic activity 1834-37
Regional volcanic activity 1719to 1790
Strong Reflection
successive flood deposits (f1-5)
f1
f2
f3
f4
f5
AD 1960 earthquake-induced mega flood deposit
AD 1960 reworked pumices
erosive base
tephra
T-I -5
T-I -5'
(1) Boës & Fagel, in press
(2) Chapron et al., in press

A discussion of the validity of these models lies beyond the scope of this article. In every respect, a post-AD 1834 age can be deduced for MWE1, with the associated MWDs located above the mentioned high-amplitude reflection. A 0.3–0.4 ms (~25–30 cm) thick drape of background sediments lies on top of the MWDs associated with MWE1. The AD 1960 event deposit is located between 15 and 30 cm or between 18 and 50 cm depth in core PU-I (according to the chosen model). Taking into account the limitations of the vertical seismic resolution and possible compaction effects during coring, it is likely that this sediment drape in the core and on seismic profiles has a similar thickness. Therefore, we can estimate the age of MWE1 at AD 1960, a period when geodynamic activity was very high in the region (Chapron et al., in press): M_w=9.5 Valdivia earthquake, landsliding, successive river floods and the Cordon–Caulle eruption. No other seismic horizons can be identified beneath the MWD due to limited acoustic penetration through the probably coarse-grained mass-wasting deposit (sediment source proximal to the Golgol River).

Fig. 6C shows another type of deposit associated with MWE1: i.e. an almost transparent onlapping lens with a ponded geometry, intercalated between draping "background sediment" reflections. This type of deposit has all characteristics of a lacustrine homogenite (Chapron et al., 1999).

6.2. MWE2

Only 4 MWD bodies are observed at this seismic–stratigraphic horizon. All are located in the Eastern Basin. They consist of elongate, lenticular units, characterized by a transparent acoustic facies and smooth upper and lower boundaries. By extrapolation of the background sedimentation rate in core PU-I and excluding visible event deposits (on seismic sections), an age of about AD 1530 is obtained for this MWE. The real age is probably younger, because of the likely presence of abundant smaller-scale event deposits (i.e. tephra deposits) in the sedimentary sequence.

6.3. MWE3 – most extensive MWE

At least 29 MWD bodies are observed at this seismic–stratigraphic horizon. They occur at the base of all slopes that are susceptible to sediment instability. At the base of the eastern ridge, acoustic penetration is too limited to observe possible MWE3 deposits. Fig. 6A shows 4 MWDs at this horizon, in transverse (MWD3(1) and MWD3(2)) and longitudinal (MWD3(3) and MWD3(4)) cross-section, as evidenced by crossing profiles.

Fig. 6C shows 2 coeval mass-wasting deposits. MWD3(2) is characterized by a chaotic to transparent facies and shows a locally continuous internal reflection. It is 180 m wide and has a maximum thickness of 1.2 m. MWD3(3) is characterised by an overall chaotic facies. It is 80 m long and has a maximum thickness of about 1 m. Fig. 6C also shows the association of these MWDs with a transparent onlapping wedge that shows a ponded geometry and a maximum thickness of 0.5 m. This unit is interpreted as the characteristic homogenous unit of a homogenite. A continuous high-amplitude reflection terminates at the rim of the MWD and directly underlies the homogenous unit. This reflection most likely represents the acoustic signature of the basal coarse-grained unit of the homogenite, by analogy with ground-truthed homogenite deposits in Lake Icalma (Bertrand et al., in press). The age of MWE3 has been calculated as about 1660 cal yr BP by interpolation between seismochronostratigraphic horizons.

Core PU-II shows some *in situ*-deformed liquefaction structures in a tephra layer (7.5 cm thick) at 1.1 m depth. Dating using the age–depth model of PU-II (Fig. 5) gives an age of ~1680 cal yr BP, which is only slightly older than the age estimated for MWE3. These *in situ* deformations can therefore be attributed to MWE3.

6.4. MWE4/5/6/7/8/9

Due to acoustic penetration limitations in most of the basin, mass-wasting deposits attributed to MWE4/5/6/7/8/9 could only be observed in the gully depression between Fresia Island and the southern platform (Fig. 2). Fig. 8 illustrates the vertical succession of mass-wasting deposits at the base of each slope of this gully depression. Respectively 4, 11, 8, 9, 5 and 7 MWDs could be mapped for MWE4, MWE5, MWE6, MWE7, MWE8 and MWE9. The age of these events is calculated to ~3730, ~4500, ~5150, ~6320, ~7510 and ~9500 cal yr BP, respectively, by interpolation between seismic chronostratigraphic horizons.

Fig. 7. (A) Example of a huge MWD (attributed to MWE1) on the foot of the Eastern Ridge. Down-warping of lower stratification probably results from consolidation of lower sediments by gravity-loading of the MWD. (B) Mass-wasting deposits (MWD) associated with MWE1/2/3 in the NE part of the Eastern Basin. These events are related to severe seismic shaking in respectively AD 1960, AD 1575 and AD 290. (C) PU-I core descriptions and age models: 1) Boës and Fagel (in press).; 2) Chapron et al. (in press). The continuous very high-amplitude reflector on panels C1 and C2 likely correlates with a pumice deposit in core PU-I (Chapron et al., in press).

7. Fluid-escape structures

On Fig. 6B, the lowermost mass-wasting deposit (MWD9) can be discriminated thanks to a number of remarkable characteristics. Its upper boundary either consists of chaotic reflections or is not discernable at all. The overlying seismic horizons are curved upward. The curvature decreases in an upward direction but is still visible in the lake-floor topography (Fig. 6A). The lateral transition between relatively flat-lying horizons and curved horizons takes place via a series of vertical acoustic anomalies with a transparent facies.

These vertical anomalies and uplifting are interpreted as fluid escape structures, possibly also involving a certain amount of sub-surface sediment mobilization, initiated during post-depositional seismic loading and liquefaction. Coseismic phenomena, such as hydraulic fracturing, lateral spreading or surface oscillations (Obermeier et al., 2005) may have initiated escape of overpressured pore-water and suspension of sediments (fluidization). This upward fluid and/or sediment transport induced the typical upwarping of the overlying stratification. Only MWD9 bears large-scale escape structures due to its greater thickness, an important factor in determining the susceptibility to liquefaction and the thickness of cap or overburden that can be penetrated (Obermeier et al., 2005). It is remarkable that the top of the fluid escape columns is located at the same stratigraphic level as the distal parts of MWD5 or MWD8, which points towards a synchroneity of sediment fluidization and slope failure. These typical "upwarping" escape structures are easily discriminated from well-known fluid expulsion depressions such as pockmarks (expulsion craters). Some small pockmarks are observed in the stratigraphic sequences from the Western Basin.

8. Discussion

8.1. Arguments for a seismic triggering of MWE in Lake Puyehue

8.1.1. Mass wasting occurs as distinct events

The occurrence of distinct mass-wasting events implies that strong regional-scale triggering mechanisms are particularly important, so that local triggers can mostly be ignored. It has been shown from historical records that synchroneity of multiple slope failures on

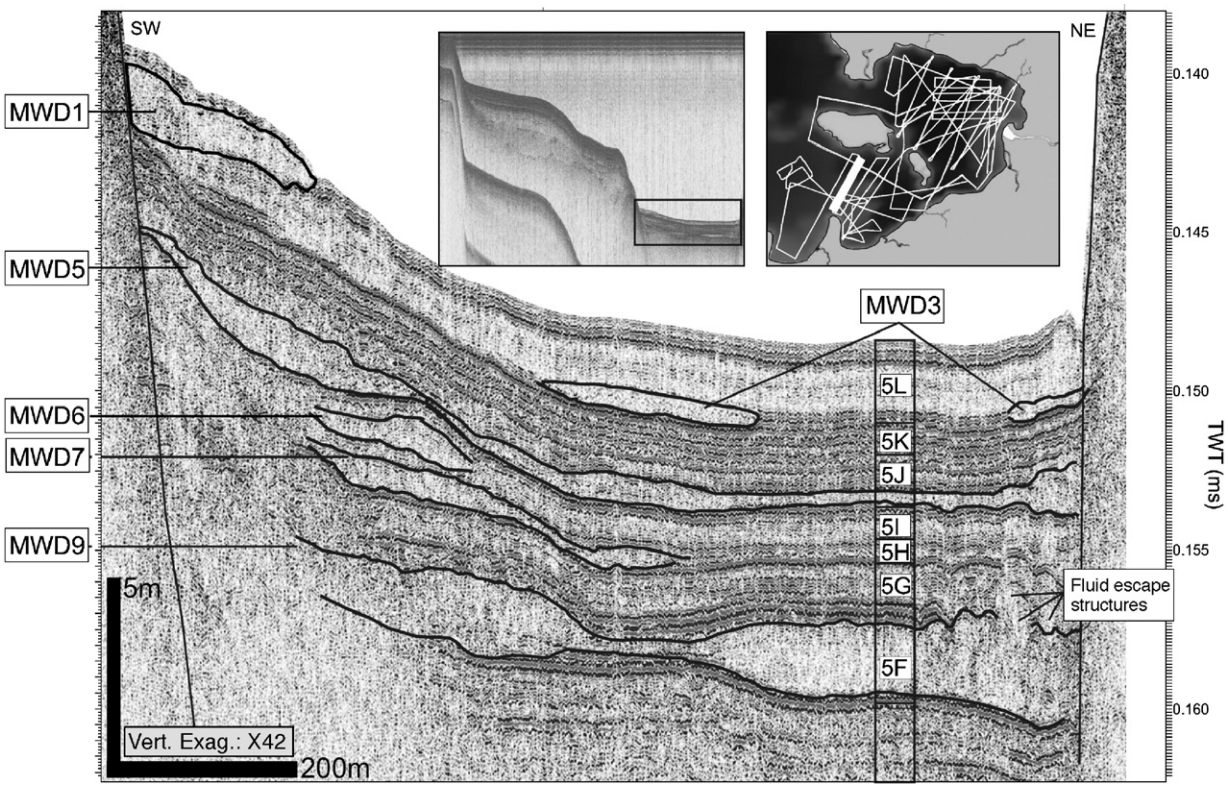

Fig. 8. Vertical succession of MWD in the gully depression, which were most likely triggered by giant earthquakes. Note some fluid escape structures originating in the northern MWE9 deposit. Seismic sub-units are indicated as in Fig. 5.

various slope angles is a common effect of strong earthquakes, both in subaerial (Keefer, 1984; Jibson, 1996; Becker and Davenport, 2003) and in lacustrine environments (Schnellmann et al., 2002). Consequently, strong historical and prehistorical earthquakes very likely triggered the most prominent mass-wasting events (MWE1, MWE3 and MWE9) in Lake Puyehue, as indicated by the numerous mass-wasting deposits at the same seismic–stratigraphic level. Seismic triggering can also be proposed, but with a lower level of confidence, for those mass-wasting events involving only a few small MWDs (e.g. MWE4).

8.1.2. Correlation of mass-wasting events and historical earthquakes

South-Central Chile's historical earthquake record indicates that the AD 1960 Valdivia earthquake (M_w=9.5) had the largest local earthquake intensity and, as a consequence, had the highest potential to be the trigger of the massive MWE1. This earthquake also triggered numerous landslides in the Golgol Valley (Chapron et al., in press) and a seiche on Lake Puyehue reaching amplitudes of about 60 cm (Veyl, 1961). This seiche probably formed the homogenite that occurs in association with the MWE1 deposits.

Other event deposits related to the AD 1960 Valdivia earthquake can also be observed in cores PU-I and PU-II, at approximately the same stratigraphic position as MWE1:

- Core PU-I (Fig. 7C1) shows a seismite (15.5 cm thick) of displaced and mixed lake deposits with deltaic material (Boës and Fagel, in press). Chapron et al. (in press) (Fig. 7C2) interpreted this unit as the upper part of a mega-flood deposit. This flood is interpreted to have been induced by successive outbursts from breached landslide dams in the course of the upstream Golgol River. Several smaller flood deposits directly overlie the AD 1960 seismite/mega-flood deposit. These flood deposits are assumed to have been induced by winter rains that washed out the (AD 1960) earthquake-triggered landslides in the Golgol Valley (Chapron et al., in press).
- Core PU-II contains a mixed layer (3.5 cm thick) resulting from sediment remobilisation (Bertrand, 2005).

MWE1 is most likely related to all these event deposits which represent the lacustrine fingerprint of the AD 1960 Valdivia earthquake. This indicates that such powerful seismic events not only cause numerous sub-lacustrine slope failures, but may also induce variations in terrigenous supply to the basin due to intensive landscape changes in the catchment (Jibson, 1996; Keefer, 1999; Chapron et al., in press).

The 1940 and 1920 seismic events (M_w=7 and 7.4) are recorded as 0.2 cm and 0.5 cm thick terrigenous layers in core PU-II (Boës and Fagel, in press). No traces of these events have been observed on seismic profiles because their thickness is far below seismic resolution. Based on its calculated age, MWE2 can most likely be attributed to the giant AD 1575 earthquake, intensity reports of which are quite similar to those of the AD 1960 earthquake (Cisternas et al., 2005). A thin event deposit (turbidite?) is observed in core PU-II at this level, while core PU-I does not contain pre-AD 1700 sediments. Other strong historical earthquakes, such as the AD 1737 ($M_s \approx 7.5$) and AD 1837 ($M_s \approx 8$) earthquakes (Lomnitz, 2004), did not provoke any obvious sediment disturbances in Lake Puyehue.

8.1.3. Slope failure mechanism: sediment characteristics, slope angle, ground motion

The sedimentary sequence on the platform (core PU-II) mainly consists of silts intercalated with 79 coarser-grained tephra layers and 3 turbidites. During seismic loading, excess pore-pressure accumulation under a permeability barrier could cause liquefaction in these intercalated coarser-grained materials (Zeghal et al., 1999), which could locally reduce the strength of the sand–silt sedimentary column. Therefore, these intercalated coarse layers could act as a "weak" layer on which sliding failures could develop (Biscontin and Pestana, 2006). The steeper the slope angle, the larger the accumulated downhill strain at the end of seismic shaking (Biscontin and Pestana, 2006). In case of the platform South of the gully depression, it thus can be assumed that seismic slope failure preferentially develops at the slope break between the "stable" sediments of the platform (slope: 0°–2°) and "unstable" sediments on the steep slopes (slope: 10°–25°) bordering the gully depression. In general, seismic ground motions with a long duration and a low frequency content, such as those caused by strong, distant earthquakes, cause more significant excess pore pressure and thus tend to be more detrimental for slope stability (Leynaud et al., 2004; Biscontin and Pestana, 2006). This favors the development of multiple slope failures during giant 1960-like earthquakes with origin at the distant subduction interface.

8.1.4. The link with homogenites

Lacustrine homogenite deposits are most often attributed to seiche processes. A seiche is an oscillation of the lake water body, resulting from direct seismic

wave impact or (earthquake-triggered?) mass-movements (e.g. Siegenthaler et al., 1987; Chapron et al., 1999; Bertrand et al., in press). The water movement allows the suspension of fine-grained material and its massive settling when the oscillation wanes. On very high resolution seismic profiles, such a seiche deposit, or homogenite, appears as a mostly transparent unit, ponded in the deepest parts of the lake (e.g. Bertrand et al., in press). In Lake Puyehue, homogenites were observed at the same stratigraphic horizon as MWE1 and MWE3, indicating the enormous impact of these MWEs and the likelihood of their triggering by large earthquakes.

8.1.5. Synchroneity of sediment fluidization and slope failure

Buried sediment blows are widely used as indicators of past seismic events (Obermeier, 1996). Considering South-Central Chile's prominent seismicity, the observed escape structures in Lake Puyehue (Fig. 6) are likely to have been induced by past earthquakes. Some mass-wasting events occurred simultaneously with these fluidization processes, which provides an extra indication of a seismic triggering for these mass-wasting events. It is likely that the longest escape column (Fig. 6) may have been caused by a polyphase escape, as it experienced several earthquakes.

8.1.6. Exclusion of other trigger mechanisms

In order to further test the earthquake-trigger hypothesis, we analyzed the local characteristics of areas characterized by slope failure and mass-movement deposits, such as the gully depression with its high abundance of mass-wasting deposits (Fig. 8). The borders of the gully depression are characterized by calm background sedimentation, similar to that at the PU-II coring site. These borders are located at a significant distance from any terrigenous fluvial input, eliminating *rapid slope oversteepening* on a Gilbert-type delta due to high sediment input as a possible trigger mechanism of MWEs. Slope failure occurs on every edge of the gully depression (N–W–S), which is only in the north sub-aerially bordered by Fresia Island. On the west and south margins, slope instabilities are triggered at depths of about 80 m, ruling out all kinds of shallow-water trigger mechanisms such as *wave action during storms* and *lake-level fluctuations*. Furthermore, no evidence of significant lake-level fluctuations has been found on the seismic profiles. No traces of *sub-aerial mass-movements* at the outer lake borders were observed during fieldwork in November 2004 and these would not be able to reach the gully depression anyway. Fresia Island consists of hard intrusive rocks (diorite) and is covered by dense vegetation, decreasing its potential for sub-aerial slope failure. Seismic profiles and core PU-II show no evidence of the presence of free gas in the sediments on the southern platform. This eliminates the possibility of a *sudden gas discharge* through slope sediments as a possible trigger mechanism.

Based on all above arguments and considerations, we submit that severe seismic shaking is the most plausible cause of slope failure in the gully depression. In other areas, located in the vicinity of a direct clastic input (e.g. river deltas), a seismic trigger mechanism is still very likely, although local trigger factors cannot be completely ruled out.

8.2. Quantitative paleoseismological approach?

It is generally assumed that the number of seismically triggered (subaerial) slope failures is roughly proportional to earthquake intensity (Keefer, 1984). This opens the possibility of estimating paleointensities and/or lake-epicenter distances. However, numerous other factors may also influence the type, distribution and size of earthquake-induced mass-movements. These include some seismological factors, such as ground shaking amplitude (i.e. peak horizontal ground acceleration; Kastens, 1984), the shaking duration and shaking frequency (Biscontin and Pestana, 2006). Furthermore, geotechnical sediment properties, slope angles and intensity-increasing site effects may play an important role. When comparing numbers of mass-wasting deposits, one has also to bear in mind the decrease in acoustic penetration in seismic data with increasing depth. For example: the large extent of MWE3 (29 MWD bodies) is still underestimated compared to MWE1 (17 MWD bodies) because of limited penetration at the foot of the eastern sub-lacustrine ridge, a principal mass-wasting area.

From all historical known earthquakes in South-Central Chile, only the AD 1960 Valdivia earthquake could be traced in Lake Puyehue by the presence of seismites in two cores, by numerous mass-wasting deposits and by a homogenite deposit, indicating its exceptional strength. No mass-wasting deposits were observed in association with the significant AD 1737 and AD 1837 earthquakes, indicating that these seismic events were less severe or had a larger epicenter-lake distance. This observation is confirmed by other paleoseismic investigations in South-Central Chile, based on the succession of seismogenic tsunami deposits and paleosols (Cisternas et al., 2005).

It is remarkable that our study identified only 4 mass-wasting deposits associated with the AD 1575

earthquake, although historical records reveal similar effects to those from the AD 1960 Valdivia earthquake (Lomnitz, 1970, 2004; Cisternas et al., 2005). This apparent contradiction possibly illustrates the problems arising with the veracity of historical earthquake intensity reports (Lomnitz, 2004). Another possibility is that Lake Puyehue's depositional processes and history also exerted a strong influence on the capacities of the sedimentary archive to record earthquake effects. As indicated by the age–depth model (Fig. 5), the period 3000–500 cal yr BP is characterised by a relatively low mean sedimentation rate of about 0.36 mm/yr (period before: 0.87 mm/yr; period after: 1.58 mm/yr). Potentially unstable slope sediments were removed during the strong earthquake associated with the extensive MWE3, at about 1660 cal yr BP (AD 290). New slope sediments probably accumulated too slowly to become unstable during the great AD 1575 earthquake, so that this major earthquake could only generate a few MWD. Furthermore, the latter occurred in the Eastern Basin, on locations with the highest sedimentation rates (e.g. proximal to the Golgol River inflow). A detailed inter-lake basin study of depositional history effects on lacustrine earthquake recording is therefore required before attempting to adopt a quantitative paleo-earthquake approach.

8.3. Paleoseismological reconstruction for giant earthquakes in South-Central Chile

The postulation of strong earthquakes as the most likely triggers of the observed mass-wasting events in Lake Puyehue allows us to make a rough paleoseismological reconstruction of giant earthquake occurrences in South-Central Chile, for the last 10,000 yr (Fig. 9). The right-hand column in Fig. 9 gives a qualitative assessment of the degree of confidence with regard to the seismic origin of the MWE.

Evaluation of historical earthquakes has indicated that the sedimentary archive of Lake Puyehue only records giant seismic events with ground-shaking comparable to the AD 1960 and AD 1575 earthquake. This is analogous to the record of buried soils and tsunami deposits studied by Cisternas et al. (2005). For prehistorical earthquakes, no correlations could be achieved. Our paleoseismic record reveals the occurrence of 9 giant earthquakes during the Holocene, which is strikingly comparable to the 8–10 Holocene seismic events revealed by the study of marine turbidites at ODP-site 1232 offshore Valdivia (Blumberg et al., personal communication). Detailed correlations could not be achieved due to dating problems of the marine

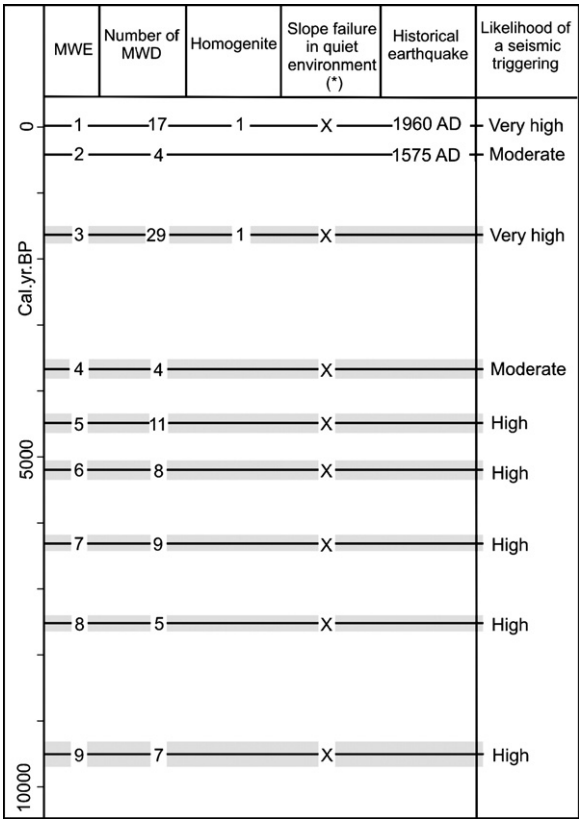

Fig. 9. Temporal distribution of the mass-wasting events and their paleoseismological significance. Shadings indicate minimum error bars (only considering ^{14}C inaccuracies). (*) This column indicates whether slope failure occurred in quiet depositional environments, for example the slopes of the gully depression. These are characterized by a quasi-continuous sedimentation rate and slope failures at water depths >40 m.

turbidites. The seismic recurrence interval in our reconstruction varies between 500 and 2000 yr with an average of ~1000 yr, which is rather large compared to the 285 yr average recurrence rate in Cisternas et al. (2005). This could possible be due to time-variable earthquake-recording capacities (creation and preservation thresholds) of the studied paleoseismic records (e.g. Nelson et al., 2006). Paleoseismological reconstructions for other subduction zones also show smaller recurrence intervals (e.g. Cascadia: 400–600 yr; Adams, 1990; Goldfinger et al., 2003; Karlin et al., 2004; Nelson et al., 2006). However, periods without mass-wasting events (e.g. 1700–3700 cal yr BP) should not necessarily be interpreted as periods without very strong earthquakes, as the apparent quiescence can also reflect a temporary lack of potentially unstable slope sediments (e.g. Kastens, 1984; Beck et al., 1996; Beck et al., 2005) due to (climatic or volcanically induced) variations in sediment input. For the lacustrine environment, a

thorough comparison and correlation of paleoseismic records in several South-Chilean lakes should allow these local earthquake-recording characteristics to be eliminated, facilitating a complete, consistent paleoseismic reconstruction for strong earthquakes.

The recurrence interval of large historical earthquakes along the Valdivia rupture zone is about ~128 yr. Such a recurrence rate is, however, too short to explain the giant AD 1960 earthquake, the slip of which required about 250–350 yrs of plate motion (Cifuentes, 1989; Cisternas et al., 2005). This implies that not all of the accumulated strain is released in every earthquake, and that giant earthquakes (i.e. those recorded in the lacustrine sedimentary archives) only occur sporadically, embedded in a series of "normal" earthquakes (i.e. not recorded in lacustrine sedimentary archives). Such a variable rupture behavior has also been proposed for other subduction zones worldwide (e.g. Kanamori and McNally, 1982; Nelson et al., 2006).

One also has to be cautious with interpretations of South-Central Chile's paleoseismicity because of the possibility for large earthquakes that are not generated by underthrusting processes. For example, the destructive AD 1939 Chilean earthquake (36.25°S; Concepcion Rupture Zone) was a complex normal-fault earthquake in the down-going oceanic slab (Beck et al., 1998). Such intra-slab earthquakes have occurred in different parts of Chile (Campos et al., 2002), and must thus be taken into account in any paleoseismological analysis.

9. Conclusions

Very high resolution reflection seismic profiling illustrated that the sedimentary fill of South-Central Chile's glacigenic lakes represent a continuous and easily-datable archive of past strong earthquakes. Combined high-resolution reflection seismic profiling and sediment coring allows identification and dating of seismically triggered mass-wasting deposits, and determination of their geographical and temporal distribution.

In Lake Puyehue, analysis of very high resolution seismic profiles yielded nine significant mass-wasting events. All mass-wasting events are characterized by multiple coeval mass-movement deposits, and some are associated with homogenite deposits. The youngest of these recorded events represents the devastating AD 1960 Valdivia earthquake (M_w=9.5). Also for the 8 other mass-wasting events, a seismic trigger by strong earthquakes seems most likely.

Quantitative comparison of mass-wasting events related to historical known earthquakes highlights the influence of volcanically- or climatically-induced variations in sediment accumulation rate on the potential for slope failure. This probably causes the striking contrast in number of mass-wasting deposits (17 versus 4) between the AD 1960 and AD 1575 earthquakes, the historical intensity reports of which suggest they were of comparable magnitude.

A paleoseismological reconstruction yields a recurrence rate for giant earthquakes (AD 1960-like earthquakes) in the Valdivia region of 500 to 2000 yrs. Periods without mass-wasting events can reflect the absence of very strong earthquakes due to e.g. changes in the interplate coupling processes, or they can be explained by the temporary lack of potentially unstable slope sediments.

Our paleoseismological reconstruction has to be improved by adding additional lacustrine archives from the area and by comparing with other paleoseismological archives, such as liquefaction structures, tree-ring disturbances, marine turbidites, buried soils and tsunami deposits. Such a thorough paleoseismological reconstruction, combined with historical and instrumental data, will provide the background data required for a reliable seismic-hazard assessment for South-Central Chile.

Acknowledgements

We thank Alejandro Peña, Waldo San Martin and Koen De Rycker for their logistic and technical support of the seismic surveys of 2001–2002 and 2004 and Juan Luis Garcia for help during fieldwork and interesting discussions. We would also like to thank the whole ENSO-CHILE team for stimulating discussions, and sharing of data and ideas. This work was financially supported by the Belgian SSTC project EV/12/10B "A continuous Holocene record of ENSO variability in southern Chile" and by the Flemish–Chilean bilateral scientific collaboration project "Impacts of volcanic activity, climate and land cover changes on the ecology and watershed hydrology of Andean lakes in Southern Central Chile". The contribution of M. Pino was financially supported by the Chilean project FORECOS P04-065F from the Millennium Initiative (MIDEPLAN). J. Moernaut acknowledges the support of the Institute for the Promotion of Innovation through Science and Technology in Flanders (IWT-Vlaanderen). We thank two anonymous reviewers for constructive reviews of the manuscript.

References

Adams, J., 1990. Paleoseismicity of the Cascadia subduction zone – evidence from turbidites off the Oregon–Washington margin. Tectonics 9 (4), 569–583.

Beck, C., Manalt, F., Chapron, E., Van Rensbergen, P., De Batist, M., 1996. Enhanced seismicity in the early post-glacial period: evidence from the post-Würm sediments of Lake Annecy, northwestern Alps. Journal of Geodynamics 22, 155–171.

Beck, C., Schneider, J.-L., Mercier de Lépinay, B., Cremer, M., Çağatay, N., Boutareaud, S., Schmidt, S., Weber, O., Armijo, R., Pondard, N., MARMACORE Scientific Party, 2005. Co-seismic sedimentation during the last lacustrine stage of the Sea of Marmara, North-Anatolian Fault, Turkey. EGU meeting Vienna. Geophysical research abstracts, vol. 7. abstract nr. 09050.

Beck, S., Barrientos, S., Kausel, E., Reyes, M., 1998. Source characteristics of historic earthquakes along the central Chile subduction zone. Journal of South American Earth Sciences 11 (2), 115–129.

Becker, A., Davenport, C.A., 2003. Rockfalls triggered by the AD 1356 Basle earthquake. Terra Nova 15, 258–264.

Bentley, M.J., 1997. Relative and radiocarbon chronology of two former glaciers in the Chilean Lake District. Journal of Quaternary Science 12, 25–33.

Bertrand, S., 2002. Caractérisation des apports sédimentaires lacustres de la region des lacs, Chili méridional (exemple des lacs Icalma et Puyehue). Mémoire de DEA. Université de Liège.

Bertrand, S., 2005. Sédimentation lacustre postérieure au dernier maximum glaciaire dans les lacs Icalma et Puyehue (Chili meridional): réconstitution de la variabilité climatique et des évènements sismo-tectoniques. Ph.D. Thesis, Université de Liège.

Bertrand, S., Charlet, F., Fagel, N., De Batist, M., Chapron, E., in press. Reconstruction of the Holocene seismo-tectonic activity of the Southern Andes form seismites recorded in Lago Icalma, Chile, 39°S. Palaeogeography, Palaeoclimatology, Palaeoecology.

Biscontin, G., Pestana, J.M., 2006. Factors affecting seismic response of submarine slopes. Natural Hazards and Earth System Sciences 6, 97–107.

Boës, X., Fagel, N., in press. Climate-varve significance in Southern Chile (Lago Puyehue, 40°S). Journal of Paleolimnology.

Bohm, M.L.S., Echtler, H., Asch, G., Bataille, K., Bruhn, C., Rietbrock, A., Wigger, P., 2002. The Southern Andes between 36° and 40°S latitude: seismicity and average seismic velocities. Tectonophysics 356, 275–289.

Bookhagen, B., Echtler, H.P., Melnick, D., Strecker, M.R., Spencer, J.Q.J., 2006. Using uplifted Holocene beach berms for paleoseismic analysis on the Santa María Island, south-central Chile. Geophysical Research Letters 33, L15302, doi:10.1029/2006GL026734.

Campos, H.S.W., Agüero, G., Parra, O., Zúñiga, L., 1989. Estudios` limnologicos en el Lago Puyehue (Chile): Morfometria, factores fisicos y quimicos, plancton y productividad primaria. Medio Ambiente 10 (2), 36–53.

Campos, J.H.D., Madariaga, R., Lopez, G., Kausel, E., Zollo, A., Iannacone, G., Fromm, R., Barrientos, S., Lyon-Caen, H., 2002. A seismological study of the 1835 seismic gap in south-central Chile. Physics of the Earth and Planetary Interiors 132, 177–195.

Cembrano, J., Schermer, E., Lavenu, A., Sanhueza, A., 2000. Contrasting nature of deformation along an intra-arc shear zone, the Liquiñe–Ofqui fault zone, southern Chilean Andes. Tectonophysics 319, 129–149.

Chapron, E., Beck, C., Pourchet, M., Deconinck, J.-F., 1999. 1822 earthquake-triggered homogenite in Lake Le Bourget (NW Alps). Terra. Nova 11 (2/3), 86–92.

Chapron, E., Ariztegui, D., Mulsow, S., Villarosa, G., Pino, M., Outes, V., Juvignié, E., Crivelli, E., in press. Impact of the 1960 major subduction earthquake in Northern Patagonia (Chile, Argentina). Quaternary International.

Charlet, F., Chapron, E., De Batist, M., Pino, M., Urrutia, R., submitted for publication. Seismic stratigraphy of Lago Puyehue (Chilean Lake District): new views on its deglacial and Holocene evolution. Journal of Paleolimnology.

Cifuentes, I.L., 1989. The 1960 Chilean earthquakes. Journal of Geophysical Research 94, 665–680.

Cisternas, M., Atwater, B.F., Torrejon, F., Sawai, Y., Machucha, G., Lagos, M., Eipert, A., Youlton, C., Salgado, I., Kamataki, T., Shishikura, M., Rajendran, C.P., Malik, J.K., Rizal, Y., Husni, M., 2005. Predecessors of the giant 1960 Chile earthquake. Nature 437, 404–407.

De Mets, C., Gordon, R.G., Argus, D.G., Stein, S., 1994. Effect of recent revisions to the geomagnetic reversal time scale on estimate of current plate motions. Geophysical Research Letters 21, 2191–2194.

Doig, R., 1986. A method for determining the frequency of large-magnitude earthquakes using lake sediments. Canadian Journal of Earth Sciences 23, 930–937.

Duke, C.M., Leeds, D.J., 1963. Response of soils, foundations, and earth structures to the Chilean earthquakes of 1960. Bulletin of the Seismological Society of America 53 (2), 309–357.

Ettensohn, F.R., Kulp, M.A., Rast, N., 2002. Interpreting ancient marine seismites and apparent epicentral areas for paleo-earthquakes, Middle Ordovician Lexington Limestone, central Kentucky. In: Ettensohn, F.R., Rast, N., Brett, C.E. (Eds.), Ancient Seismites. Geological Society of America Special Paper, 359, pp. 177–190.

Finckh, P., Kelts, K., Lambert, A., 1984. Seismic stratigraphy and bedrock forms in perialpine lakes. Geological Society of America Bulletin 95, 1118–1128.

Gerlach, D.C., F.F.A., Moreno-Roa, H., Lopez-Escobar, L., 1988. Recent volcanism in the Puyehue–Cordon Caulle region, southern Andes, Chile (40.5°S): petrogenesis of evolved lavas. Journal of Petrology 29 (2), 333–382.

Goldfinger, C., Nelson, C.H., Johnson, J.E., 2003. Holocene earthquake records from the Cascadia subduction zone and northern San Andreas Fault based on precise dating of offshore turbidites. Annual Review of Earth and Planetary Sciences 31, 555–577.

Green, R.A., Obermeier, S.F., Olson, S.M., 2005. Engineering geologic and geotechnical analysis of paleoseismic shaking using liquefaction effects: field examples. Engineering Geology 76, 263–293.

Heirman, K., 2005. Reconstructie van de deglaciatiegeschiedenis in het gebied van Lago Puyehue, zuidelijk Chili, aan de hand van seismische profielen en veldwaarnemingen. M.Sc. thesis, UGent. 167 pp.

Inouchi, Y., Kinugasa, Y., Kumon, F., Nakano, S., Yasumatsu, S., Shiki, T., 1996. Turbidites as records of intense palaeoearthquakes in Lake Biwa, Japan. Sedimentary Geology 104, 117–125.

Ishihara, K., 1985. Stability of natural soils during earthquakes. Proc. the Eleventh International Conference on Soil Mechanics and Foundation Engineering, San Francisco, vol. 1. A.A. Balkema, Rotterdam, pp. 321–376.

Ishii, M., Shearer, P.M., Houston, H., Vidale, J.E., 2005. Extent, duration and speed of the 2004 Sumatra–Andaman earthquake imaged by the Hi-Net array. Nature 435, 933–936.

Jibson, R.W., 1996. Use of landslides for paleoseismic analysis. Engineering Geology 43, 291–323.

Jordan, T.E., Burns, W.M., Veiga, R., Pangaro, F., Copeland, P., Kelley, S., Mpodozis, C., 2001. Extension and basin formation in the southern Andes caused by increased convergence rate: a mid-Cenozoic trigger for the Andes. Tectonics 20 (3), 308–324.

Kanamori, H., McNally, K.C., 1982. Variable rupture mode of the subduction zone along the Ecuador–Colombia coast. Bulletin of the Seismological Society of America 72, 1241–1253.

Karlin, R.E., Holmes, M., Abella, S.E.B., Sylwester, R., 2004. Holocene landslides and a 3500-year record of Pacific Northwest earthquakes from sediments in Lake Washington. Geological Society of America Bulletin 116, 94–108.

Kastens, K.A., 1984. Earthquakes as a triggering mechanism for debris flows and turbidites on the Calabrian Ridge. Marine Geology 55, 13–33.

Keefer, D.K., 1984. Landslides caused by earthquakes. Geological Society of America Bulletin 95, 406–421.

Keefer, D.K., 1999. Earthquake-induced landslides and their effects on alluvial fans. Journal of Sedimentary Research 69 (1), 84–104.

Kelleher, J.A., 1972. Rupture zones of large South American earthquakes and some predictions. Journal of Geophysical Research 77 (11), 2087–2103.

Klotz, J., Khazaradze, G., Angermann, D., Reigber, C., Perdomo, R., Cifuentes, O., 2001. Earthquake cycle dominates contemporary crustal deformation in Central and Southern Andes. Earth and Planetary Science Letters 193, 473–446.

Lara, L.E., Naranjo, J.A., Moreno, H., 2004. Rhyodacitic fissure eruption in Southern Andes (Cordon Caulle; 40.5°S) after the 1960 (M_w: 9.5) Chilean earthquake: a structural interpretation. Journal of Volcanology and Geothermal Research 138, 127–138.

Laugenie, C., 1982. La région des lacs, Chili méridional. PhD thesis. Université de Bordeaux III, 822 p.

Lavenu, A., Cembrano, J., 1999. Compressional- and transpressional-stress pattern for Pliocene and Quaternary brittle deformation in fore arc and intra-arc zones (Andes of Central and Southern Chile). Journal of Structural Geology 21, 1669–1691.

Leynaud, D., Mienert, J., Nadim, F., 2004. Slope stability assessment of the Helland Hansen area offshore the mid-Norwegian margin. Marine Geology 213, 457–480.

Lomnitz, C., 1970. Major earthquakes and tsunamis in Chile during the period 1535 to 1955. Geologische Rundschau 59, 938–960.

Lomnitz, C., 2004. Major earthquakes of Chile: a historical survey, 1535–1960. Seismological Research Letters 75, 368–378.

Lorenzo-Martin, F., Roth, F., Wang, R., 2006. Inversion for rheological parameters from post-seismic surface deformation associated with the 1960 Valdivia earthquake, Chile. Geophysical Journal International 164, 75–87.

Melnick, D., Bookhagen, B., Echtler, H.P., Strecker, M.R., in press. Coastal deformation and great subduction earthquakes, Isla Santa María, Chile (37°S). Geological Society of America Bulletin.

Moernaut, J., 2005. Lago Puyehue (zuidelijk Chili): seismische stratigrafie en detailstudie van hellingsinstabiliteiten. M.Sc. thesis, UGent, 121 pp.

Monecke, K., Flavio, S., Anselmetti, F., Becker, A., Sturm, M., Giardini, D., 2004. The record of historic earthquakes in lake sediments of Central Switzerland. Tectonophysics 394, 21–40.

Müller, R.D., Roest, W.R., Royer, J.-Y., Gahagan, L.M., Sclater, J.G., 1997. Digital isochrones of the world's ocean floor. Journal of Geophysical Research 102 (B2), 3211–3214.

Nelson, A.R., Kelsey, H.M., Witter, R.C., 2006. Great earthquakes of variable magnitude at the Cascadia subduction zone. Quaternary Research 65, 354–365.

Nishenko, S.P., 1985. Seismic potential for large and great interplate earthquakes along the Chilean and Southern Peruvian margins of South America: a quantitative reappraisal. Journal of Geophysical Research 90, 3589–3615.

Nomade, J., Chapron, E., Desmet, M., Reyss, J.L., Arnaud, F., Lignier, V., 2005. Reconstructing historical seismicity from lake sediments (Lake Laffrey, Western Alps, France). Terra Nova 17 (4), 350–357.

Obermeier, S.F., 1996. Use of liquefaction-induced features for paleoseismic analysis – an overview of how seismic liquefaction features can be distinguished from other features and how their regional distribution and properties of source sediment can be used to infer the location and strength of Holocene paleo-earthquakes. Engineering Geology 44, 1–76.

Obermeier, S.F., Olson, S.C., Green, R.A., 2005. Field occurrences of liquefaction-induced features: a primer for engineering geologic analysis of paleoseismic shaking. Engineering Geology 76, 209–234.

Pardo, M., Comte, D., Monfret, T., 2002. Seismotectonic and stress distribution in the central Chile subduction zone. Journal of South American Earth Sciences 15, 11–22.

Rapela, C.W., Pankhurst, R.J., 1992. The granites of northern Patagonia and the Gastre Fault System in relation to the break-up of Gondwana. Geological Society of Special Publication 68, 209–220.

Schnellmann, M., Anselmetti, F.S., Giardini, D., McKenzie, J.A., Ward, S.N., 2002. Prehistoric earthquake history revealed by lacustrine slump deposits. Geology 30, 1131–1134.

SERNAGEOMIN, 2003. Mapa Geológico de Chile: versión digital. Servicio Nacional de Geología y Minería, Publicación Geológica Digital 4 (CD-ROM, version 1.0, 2003). Santiago.

Siegenthaler, C., Finger, W., Kelts, K., Wang, S., 1987. Earthquake and seiche deposits in Lake Lucerne, Switzerland. Eclogae Geologicae Helveticae 80, 241–260.

Sievers, H., 2000. El maremoto del 22 mayo de 1960 en las costas de Chile, 2ª edición. Servicio Hidrográfico y Oceanográfico de la Armada de Chile. 72 pp.

Sims, J.D., 1975. Determining earthquake recurrence intervals from deformational structures in young lacustrine sediments. Tectonophysics 29, 141–152.

Stauder, W., 1973. Mechanism and spatial distribution of Chilean earthquakes with relation to subduction of the oceanic plate. Journal of Geophysical Research 78, 5033–5061.

Stern, C.R., 2004. Active Andean volcanism: its geologic and tectonic setting. Revista Geologica de Chile 31 (2), 161–206.

Veyl, C., 1961. Los sismos y las erupciones de mayo de 1960 en el sur de Chile. Boletin Sociedad Chilena de Química 11 (1–2), 20–32.

Willner, A.P., Glodny, J., Gerya, T.V., Godoy, E., Massonne, H.-J., 2004. A counterclockwise PTt path of high-pressure/low-temperature rocks from the Coastal Cordillera accretionary complex of south-central Chile: constraints for the earliest stage of subduction mass flow. Lithos 75, 283–310.

Zeghal, M., Elgamal, A.-W., Zeng, X., Arulmoli, K., 1999. Mechanism of liquefaction response in sand–silt dynamic centrifuge tests. Soil Dynamics and Earthquake Engineering 18, 71–85.